



Original article

Structure-based virtual screening of phytochemicals and repurposing of FDA approved antiviral drugs unravels lead molecules as potential inhibitors of coronavirus 3C-like protease enzyme

Arun Bahadur Gurung^{a,*}, Mohammad Ajmal Ali^b, Joongku Lee^{c,*}, Mohammad Abul Farah^d, Khalid Mashay Al-Anazi^d

^a Department of Basic Sciences and Social Sciences, North-Eastern Hill University, Shillong 793022, Meghalaya, India

^b Department of Botany and Microbiology, College of Science, King Saud University, Riyadh 11451, Saudi Arabia

^c Department of Environment and Forest Resources, Chungnam National University, 99 Daehak-ro, Yuseong-gu, Daejeon 34134, Republic of Korea

^d Genetics Laboratory, Department of Zoology, College of Science, King Saud University, Riyadh 11451, Saudi Arabia

ARTICLE INFO

Article history:

Received 13 May 2020

Revised 9 June 2020

Accepted 12 July 2020

Available online 17 July 2020

Keywords:

Coronaviruses
3C-like protease
SARS-CoV
MERS-CoV
Molecular docking
Virtual screening
FDA approved drugs
Antiviral drugs
Phytochemicals

ABSTRACT

Coronaviruses are enveloped positive-strand RNA viruses belonging to family *Coronaviridae* and order *Nidovirales* which cause infections in birds and mammals. Among the human coronaviruses, highly pathogenic ones are Severe Acute Respiratory Syndrome coronavirus (SARS-CoV) and the Middle East Respiratory Syndrome coronavirus (MERS-CoV) which have been implicated in severe respiratory syndrome in humans. There are no approved antiviral drugs or vaccines for the treatment of human CoV infection to date. The recent outbreak of new coronavirus pandemic, coronavirus disease 2019 (COVID-19) has caused a high mortality rate and infections around the world which necessitates the need for the discovery of novel anti-coronaviral drugs. Among the coronaviruses proteins, 3C-like protease (3CL^{PRO}) is an important drug target against coronaviral infection as the auto-cleavage process catalysed by the enzyme is crucial for viral maturation and replication. The present work is aimed at the identification of suitable lead molecules for the inhibition of 3CL^{PRO} enzyme via a computational screening of the Food and Drug Administration (FDA) approved antiviral drugs and phytochemicals. Based on binding energies and molecular interaction studies, we shortlisted five lead molecules (both FDA approved drugs and phytochemicals) for each enzyme targets (SARS-CoV-2 3CL^{PRO}, SARS-CoV 3CL^{PRO} and MERS-CoV 3CL^{PRO}). The lead molecules showed higher binding affinity compared to the standard inhibitors and exhibited favourable hydrophobic interactions and a good number of hydrogen bonds with their respective targets. A few promising leads with dual inhibition potential were identified among FDA approved antiviral drugs which include DB13879 (Glecaprevir), DB09102 (Daclatasvir), molecule DB09297 (Paritaprevir) and DB01072 (Atazanavir). Among the phytochemicals, 11,646,359 (Vincapusine), 120,716 (Alloyohimbine) and 10,308,017 (Gummadiol) showed triple inhibition potential against all the three targets and 102,004,710 (18-Hydroxy-3-epi-alpha-yohimbine) exhibited dual inhibition potential. Hence, the proposed lead molecules from our findings can be further investigated through *in vitro* and *in vivo* studies to develop into potential drug candidates against human coronaviral infections.

© 2020 The Author(s). Published by Elsevier B.V. on behalf of King Saud University. This is an open access article under the CC BY-NC-ND license (<http://creativecommons.org/licenses/by-nc-nd/4.0/>).

1. Introduction

Coronaviruses belong to the *Coronavirinae* subfamily, family *Coronaviridae* and order *Nidovirales*. The subfamily members based on genomic structure and phylogenetic study can be classified under four genera – *Alpha-*, *Beta-*, *Gamma-* and *Delta-coronavirus* (Cui et al., 2019). The first two genera cause infections in only mammals while birds and mammals are commonly infected by *Gamma-* and *Delta-coronaviruses* (Woo et al., 2012). While *Alpha-coronaviruses* and *Beta-coronaviruses* are known to cause gas-

* Corresponding authors.

E-mail addresses: arunbgurung@gmail.com (A. Bahadur Gurung), joongku@cnu.ac.kr (J. Lee).

Peer review under responsibility of King Saud University.



<https://doi.org/10.1016/j.jksus.2020.07.007>

1018-3647/© 2020 The Author(s). Published by Elsevier B.V. on behalf of King Saud University.

This is an open access article under the CC BY-NC-ND license (<http://creativecommons.org/licenses/by-nc-nd/4.0/>).

troenteritis in animals, in humans, they commonly cause respiratory distress (Cui et al., 2019). There are four human coronaviruses such as HCoV-229E, HKU1, HCoV-NL63 and HCoV-OC43 which induce mild upper respiratory infections and two highly pathogenic ones, such as Severe Acute Respiratory Syndrome coronavirus (SARS-CoV) and Middle East Respiratory Syndrome coronavirus (MERS-CoV) implicated in severe respiratory syndrome in humans (Forni et al., 2017; Su et al., 2016). All human coronaviruses are reported to have animal origins based on the current sequence studies, for example, SARS-CoV, MERS-CoV, HCoV-229E and HCoV-NL63 have been originated in bats while HKU1 and HCoV-OC43 are probably linked to rodents (Forni et al., 2017; Su et al., 2016). The intermediate hosts such as domestic animals may play a significant role in facilitating the easy transfer of viruses from natural hosts to humans (Cui et al., 2019). Furthermore, domestic animals themselves are susceptible to bat-borne or closely related coronavirus diseases (Lacroix et al., 2017; Simas et al., 2015). At present, 7 of 11 species of *Alpha-coronavirus* specified by the International Committee on Taxonomy of Viruses (ICTV) and 4 of 9 species of *Beta-coronavirus* have been reported only in bats. Consequently, bats are probably the main natural reservoirs of *Alpha- and Beta-coronaviruses* (Woo et al., 2012).

Coronaviruses are enveloped viruses of about 80–120 nm in diameter, with round and often pleiomorphic virions. They contain positive-strand RNA, with the largest genome (~30 kb) known till date (Lai, 2001). A helical capsid found within the viral membrane is composed of genomic RNA complexed with the basic nucleocapsid (N) protein. All coronaviruses display at least three membrane viral proteins. This includes type I glycoprotein, spike (S) protein which forms peplomers on the surface and gives a characteristic crown-like appearance, the membrane (M) protein and a small membrane protein, an envelope protein (E). All coronaviruses have a similar genomic structure (Weiss and Navas-Martin, 2005). The replicase gene located within 5' region approximately 20–22 kb encodes several enzymatic activities. The gene products of the replicase are encoded within two very large open reading frames, ORFs 1a and 1b, which are translated by a frameshift mechanism into two large polypeptides, pp1a and pp1ab (Gorbalenya, 2001; Lee et al., 1991). With the help of S protein, coronaviruses bind to their specific host cellular receptors. On gaining entry into the cell, pp1a and pp1ab are translated from the viral genome RNA, ORFs 1a and 1b (Bredenbeek et al., 1990; Brian and Baric, 2005). The ORF1a encodes a picornavirus 3C-like protease (3CL^{pro}) and one or two papain-like proteases (PL^{pro} or PLP). These proteases catalyze the processing of viral pp1a and pp1ab into the mature replicase proteins (Lee et al., 1991; Ziebuhr et al., 2001). The enzymes such as RNA-dependent RNA polymerase (RdRp), a helicase (1 1 6) and others are encoded in ORF 1b and processed from pp1ab (Gorbalenya, 2001). The metabolism of coronavirus RNA and disruption of host cell processes are believed as a result of the catalytic activities of various enzymes (Ziebuhr, 2005).

As aforementioned, SARS- and MERS-CoVs genome harbours two ORFs: ORF1a and ORF1b wherein ORF1a encodes two cysteine proteases viz: a papain-like protease (PL^{pro}) and a 3C-like protease (3CL^{pro}) also known as main protease (M^{pro}). While PL^{pro} manages cleavage on the first three cutting sites of its polyprotein, 3CL^{pro} is responsible for cleavage at other eleven positions causing the release of sixteen non-structural proteins (nsp) (Jo et al., 2020). The crystal structures of SARS- and MERS-CoVs 3CL^{pro} reveal the presence of three structural domains in each monomer wherein domains I and II has a characteristic chymotrypsin-like fold with a catalytic cysteine and are linked to a third C-terminal domain by a long loop (Needle et al., 2015). Therefore, 3CL^{pro} is an important drug target against coronaviral infection as the auto-cleavage process is indispensable for viral maturation and replication (Jo et al., 2020).

The recent outbreak of new coronavirus pandemic or coronavirus disease 2019 (COVID-19) has caused high mortality rate and infections around the world (Wu et al., 2020; Zhou et al., 2020) warrants the need for the discovery of new effective antiviral therapeutics against coronaviral infections. There are no approved antiviral drugs or vaccines for the treatment of human CoV infection to date, though many candidate therapeutics have been investigated in pre-clinical studies (Abd El-Aziz and Stockand, 2020; Dhama et al., 2020; Graham et al., 2013; Lundstrom, 2020; Padron-Regalado, 2020). Although many attempts have been previously made by workers to identify specific inhibitors for 3CL^{pro} enzymes, a few studies have been done to target all the three coronavirus protease enzymes (SARS-CoV-2 3CL^{pro}, SARS-CoV 3CL^{pro} and MERS-CoV 3CL^{pro}) using small molecules. In this study we aimed at finding suitable lead molecules for the inhibition of 3CL^{pro} enzymes through virtual screening of two chemical datasets viz: Food and Drug Administration (FDA) approved antiviral drugs and selected phytochemicals. We have proposed five lead molecules as potential inhibitors for each enzyme targets. These lead molecules could be further investigated for developing as drugs against anti-coronaviral infection.

2. Materials and methods

2.1. Selection and retrieval of phytochemicals and FDA approved drugs

A total of 263 phytochemicals and 75 FDA approved antiviral drugs were retrieved from the database of Indian Plants, Phytochemistry And Therapeutics (IMPPAT) (Mohanraj et al., 2018) and DrugBank database (Wishart et al., 2008) respectively. The three-dimensional structure of the molecules was downloaded in SDF format and the molecules whose only two-dimensional structures were available, were converted into the three-dimensional form using OpenBabel software version 2.4.1 (O'Boyle et al., 2011) and optimized using the Merck molecular force field (MMFF94) (Halgren, 1996).

2.2. Screening of drug-like compounds:

The drug-like compounds from the phytochemicals set were filtered based on Lipinski's rule of five (Lipinski, 2004), Veber's rule (Veber et al., 2002) and Adsorption, Distribution, Metabolism, Excretion and Toxicity (ADMET) physicochemical parameters. The physicochemical properties of the compounds were evaluated using DataWarrior program version 5.0 (Sander et al., 2015).

2.3. Protein-preparation

The high resolution three dimensional X-ray crystal structures of the enzyme target: SARS-CoV-2 3CL^{pro}, SARS-CoV 3CL^{pro} and MERS-CoV 3CL^{pro} were retrieved from protein data bank (PDB) (<http://www.rcsb.org/>) using their accession IDs 6Y2F, 3TNT and 5WKK at a resolution of 1.95 Å, 1.59 Å and 1.55 Å respectively. The heteroatoms including ions, cocrystal ligands (O6K, G85 and AW4 corresponding to PDB IDs: 6Y2F, 3TNT and 5WKK respectively) and water molecules were removed. Hydrogen atoms and Kolmann charges were added to the protein using AutoDockTools 1.5.6 (Morris et al., 2009) and the proteins were converted into PDBQT format.

2.4. Ligand preparation

The selected compounds were prepared for docking using AutoDockTools 1.5.6 (Morris et al., 2009). Hydrogen atoms and Gasteiger charges were added to the selected compounds and the

torsions were defined for each compound. The structures were saved in PDBQT format.

2.5. Molecular docking study

The binding affinity of each selected compound along with the control with the three enzyme targets was determined using molecular docking approach. The binding sites for the docking were defined by placing a grid box of suitable dimensions centred at each cocrystallized ligand (Table 1). Autodock Vina was used for carrying out molecular docking, which performs docking calculations based on sophisticated gradient optimization method (Trott and Olson, 2010). The binding poses were clustered and ranked in the order of their binding affinities. The molecular interactions (hydrogen bonds and hydrophobic interactions between the target proteins and compounds were studied using LigPlot + version 1.4.5 (Laskowski and Swindells, 2011).

3. Results and discussion

3.1. Virtual screening of drug-like compounds:

A set of 75 FDA approved antiviral drugs and 263 phytochemicals belonging to different classes such as prenol lipids, flavonoids, indoles and derivatives, alkaloids, lignans, organooxygen compounds etc. were used for the present study. Since the FDA approved drugs have already undergone the preclinical and clinical trials and tested safe in patients, the drugs were not tested again using *in silico* drug-like filters. While plant-derived compounds are much safer to use with fewer adverse effects, we subjected them into virtual screening protocol to reduce the drug-attrition rate. We used the rule of five (ROF) and Veber's rule filters to test the oral bioavailability of the compounds. According to ROF, a compound is considered to be orally bioactive if their physicochemical properties lie within the safe limits (molecular weight ≤ 500 Da, hydrogen bond donors ≤ 5 , hydrogen bond acceptors ≤ 10 , and an octanol–water partition coefficient $\log P \leq 5$) (Lipinski, 2004). Veber's rule states that a good oral bioavailable compound possesses number of rotatable bonds ≤ 10 and topological polar surface area $\leq 140 \text{ \AA}^2$ (Veber et al., 2002). Further, the molecules were also tested for *in silico* toxicity studies. Out of 263 phytochemicals, 46 molecules were found to be orally bioactive, non-tumorigenic, non-mutagenic, non-irritant and without any side effects on reproductive health. Thus, these 46 phytochemicals and 75 FDA approved drugs were tested further for their inhibitory potential against the three enzyme targets (Tables 2 and 3).

3.2. Top ranked lead molecules for SARS-CoV-2 3CL^{pro} from a set of phytochemicals and FDA approved drugs:

The top five leads-102004710 (18-Hydroxy-3-epi-alpha-yohimbine), 120,716 (Alloyohimbine), 10,308,017 (Gummadiol), 156798–15-1 (Asparagamine A) and 11,646,359 (Vincapusine) for SARS-CoV-2 3CL^{pro} obtained using molecular docking studies of phytochemicals showed binding energies of -8.1 kcal/mol,

-8.0 kcal/mol, -7.8 kcal/mol, -7.6 kcal/mol and -7.5 kcal/mol respectively. Molecular docking of FDA approved antiviral drugs yielded top 5 lead molecules-DB06290 (Simeprevir), DB09027 (Ledipasvir), DB09297 (Paritaprevir), DB13879 (Glecaprevir) and DB09102 (Daclatasvir) which showed binding energies of -9.7 kcal/mol, -9.3 kcal/mol, -9.3 kcal/mol, -9.3 kcal/mol and -9.2 kcal/mol respectively. The control α -ketoamide 13a inhibitor (O6K) displayed binding energy of -7.2 kcal/mol. All the lead compounds showed stable interactions with the target through a good number of hydrogen bonds as well as hydrophobic interactions except for 156798–15-1 (Asparagamine A) which exhibited only hydrophobic interactions. Interestingly, compared to the phytochemicals the FDA-approved antiviral drugs showed higher binding affinities to the target. Further, the lead molecules-10308017 (Gummadiol), 11,646,359 (Vincapusine) and DB13879 (Glecaprevir) showed the potential antiviral activity through hydrogen bond interactions with either His41 or Cys145, both of the residues constitute the catalytic dyad of SARS-CoV-2 3CL^{pro} enzyme.

3.3. Top ranked lead molecules for SARS-CoV 3CL^{pro} from a set of phytochemicals and FDA approved drugs:

Among the phytochemicals, top 5 leads-120716 (Alloyohimbine), 10,308,017 (Gummadiol), 11,646,359 (Vincapusine), 82178-34-5 (Arjunolone), 102,004,710 (18-Hydroxy-3-epi-alpha-yohimbine) showed binding energies of -9.0 kcal/mol, -8.4 kcal/mol, -8.3 kcal/mol, -8.1 kcal/mol and -8.0 kcal/mol respectively. Using molecular docking of FDA approved antiviral drugs, top 5 leads-DB13879 (Glecaprevir), DB13878 (Pibrentasvir), DB01072 (Atazanavir), DB09102 (Daclatasvir) and DB11574 (Elbasvir) were shortlisted which displayed binding energies of -9.7 kcal/mol, -9.3 kcal/mol, -9.2 kcal/mol, -9.2 kcal/mol and -8.8 kcal/mol respectively. The molecular binding between these lead compounds and the target is strengthened by a good number of hydrogen bonds and hydrophobic interactions. The leads which displayed hydrogen bond interactions with the catalytic residues-His41 and Cys145 include DB13879 (Glecaprevir), DB11574 (Elbasvir), 10,308,017 (Gummadiol) and 102,004,710 (18-Hydroxy-3-epi-alpha-yohimbine). The control, SG85 inhibitor (G85) showed binding energy of -8.0 kcal/mol with the enzyme target.

3.4. Top ranked lead molecules for MERS-CoV 3CL^{pro} from a set of phytochemicals and FDA approved drugs:

Few lead compounds were also identified for MERS-CoV 3CL^{pro} using molecular docking of phytochemicals and the binding energies of top 5 leads-11646359 (Vincapusine), 120,716 (Alloyohimbine), 10,308,017 (Gummadiol), 11,969,544 (Pericyclivine) and 28,288,759 (Vidolicine) were -9.8 kcal/mol, -8.6 kcal/mol, -8.4 kcal/mol, -8.4 kcal/mol and -8.3 kcal/mol respectively. Among, the FDA approved antiviral drugs, the top 5 leads-DB01072 (Atazanavir), DB06817 (Raltegravir), DB09296 (Ombitasvir), DB08864 (Rilpivirine) and DB09297 (Paritaprevir) scored binding energies of -9.1 kcal/mol, -9.1 kcal/mol, -9.0 kcal/mol, -8.7 kcal/mol and -8.7 kcal/mol respectively. The control,

Table 1
The grid box parameters considered for molecular docking studies.

Enzyme targets	AutoDock Vina Search Space		
	Center	Dimensions (Å)	Exhaustiveness
SARS-CoV-2 3CL ^{pro}	x: 10.9372, y: -2.0146, z: 18.2692	25 × 25 × 25	8
SARS-CoV 3CL ^{pro}	x: 25.1486, y: 44.1145, z: -5.6121	25 × 25 × 25	8
MERS-CoV 3CL ^{pro}	x: -21.9860, y: 25.6036, z: 4.0045	25 × 25 × 25	8

Table 2
List of FDA approved antiviral drugs selected for molecular docking studies.

Drugs	DrugBank ID	Therapy
Ombitasvir	DB09296	Chronic Hepatitis C
Elbasvir	DB11574	Chronic Hepatitis C
<u>Sofosbuvir</u>	DB08934	Chronic Hepatitis C
Ledipasvir	DB09027	Chronic Hepatitis C
Famciclovir	DB00426	Herpes virus infections
Simeprevir	DB06290	Chronic hepatitis C virus
Lopinavir	DB01601	Human immunodeficiency virus type 1 (HIV-1) infection.
Tecovirimat	DB12020	Smallpox
Oseltamivir	DB00198	Influenza viruses A and B infections
Baloxavir marboxil	DB13997	Influenza A and influenza B infections
Didanosine	DB00900	HIV infection
Bictegravir	DB11799	HIV-1 and HIV-2 infection
Adefovir dipivoxil	DB00718	Hepatitis B
Zalcitabine	DB00943	HIV infection
Emtricitabine	DB00879	HIV-1 infection
Zidovudine	DB00495	HIV infection
Darunavir	DB01264	HIV-1 infection
Nevirapine	DB00238	HIV-1 infection and AIDS.
Valganciclovir	DB01610	Cytomegalovirus infections
Nelfinavir	DB00220	HIV infection
Foscarnet	DB00529	cytomegalovirus retinitis, HIV infection
Boceprevir	DB08873	Chronic Hepatitis C
Inosine pranobex	DB13156	Viral infection
Dolutegravir	DB08930	HIV-1 infection
Abacavir	DB01048	HIV infection and AIDS.
Edoxudine	DB13421	Herpes simplex virus type 1 and 2 infection
Ribavirin	DB00811	Hepatitis C and viral hemorrhagic fevers
Elvitegravir	DB09101	HIV-1 infection
Amantadine	DB00915	Influenza A infection
Vidarabine	DB00194	Herpes viruses, the vaccinia virus and varicella zoster virus infection
Daclatasvir	DB09102	Hepatitis C Virus (HCV) infection
Tenofovir alafenamide	DB09299	Chronic hepatitis B and HIV-1 infection
Ritonavir	DB00503	HIV infection
Trifluridine	DB00432	Keratoconjunctivitis and recurrent epithelial keratitis
Zanamivir	DB00558	Influenza A and B virus infection
Acylovir	DB00787	Herpes simplex, <i>Varicella zoster</i> , herpes zoster infection
Ganciclovir	DB01004	AIDS-associated cytomegalovirus infections.
Entecavir	DB00442	Hepatitis B infection
Raltegravir	DB06817	HIV infection
Doravirine	DB12301	HIV-1 Infection
Pibrentasvir	DB13878	Hepatitis C virus (HCV) infection
Fosamprenavir	DB01319	HIV infection
Glecaprevir	DB13879	HCV infection
Tipranavir	DB00932	HIV infection
Etravirine	DB06414	HIV-1 infection
Amprenavir	DB00701	HIV infection.
Letermovir	DB12070	Cytomegalovirus (CMV) infection
Favipiravir	DB12466	Influenza
Idoxuridine	DB00249	Herpes simplex virus (HSV) infection
Rimantadine	DB00478	Influenza.
Tromantadine	DB13288	Herpes zoster and simplex virus infection
Telaprevir	DB05521	Chronic Hepatitis C
Dasabuvir	DB09183	Chronic Hepatitis C
Grazoprevir	DB11575	Chronic Hepatitis C
Docosanol	DB00632	HSV infection
Penciclovir	DB00299	HSV infections
Velpatasvir	DB11613	chronic Hepatitis C
Tenofovir disoproxil	DB00300	HIV infection and Hepatitis B
Cidofovir	DB00369	CMV retinitis
Voxilaprevir	DB12026	Chronic Hepatitis C
Asunaprevir	DB11586	HCV infection
Valaciclovir	DB00577	Hepatitis, HIV, and cytomegalovirus infection
Efavirenz	DB00625	HIV-1 infection
Peramivir	DB06614	Influenza A/B.
Brivudine	DB03312	Herpes zoster.
Telbivudine	DB01265	Hepatitis B virus infection
Maraviroc	DB04835	HIV infection
Stavudine	DB00649	HIV infection
Paritaprevir	DB09297	Chronic Hepatitis C
Indinavir	DB00224	HIV infection
Lamivudine	DB00709	HIV-1 and hepatitis B virus (HBV) infection
Atazanavir	DB01072	HIV infection
Rilpivirine	DB08864	HIV-1 infection
Delavirdine	DB00705	HIV-1.infection
Saquinavir	DB01232	HIV-1 and HIV-2 infection

Table 3

List of phytochemicals selected for the docking studies (MW: molecular weight; cLogP: octanol–water partition coefficient; cLogS: aqueous solubility at 25° and pH = 7.5; HBA: hydrogen bond acceptor; HBD: hydrogen bond donor; TPSA (Å²): Topological polar surface area; RB: rotatable bonds).

Molecule Name	CASID/CHEMSPIDER/ CID	Class	MW	cLogP	cLogS	HBA	HBD	TPSA	RB	Druglikeness
Heterophylloidine	78174-97-7	Prenol lipids	383.486	2.2205	-3.41	5	0	63.68	2	2.7882
Arjunolone	82178-34-5	Flavonoids	284.266	2.6114	-3.17	5	2	75.99	2	0.40331
Rosicine	95690-65-6	Indoles and derivatives	324.379	0.8137	-3.091	5	1	54.1	2	2.2389
Asparagamine A	156798-15-1	Organooxygen compounds	385.458	2.1085	-3.634	6	0	57.23	3	0.7051
Piscrocine B	752225-57-3	Heteroaromatic compounds	198.173	-0.1119	-1.262	5	3	90.9	2	0.20569
6-Acetylheteratisine	10,246,449	Quinolindines	433.543	1.1579	-3.186	7	1	85.3	4	4.6497
Gummadiol	10,308,017	Furanoid lignans	386.355	2.0507	-3.752	8	2	95.84	2	0.1606
Vidolicine	28,288,759	Indoles and derivatives	352.433	1.5661	-3.47	5	1	54.1	3	2.5754
19-Hydroxy-11-methoxytabersonine	57,619,488	Plumeran-type alkaloids	382.458	1.3822	-3.246	6	2	71.03	4	0.90699
Boldine	10,154	Aporphines	327.379	2.7882	-3.129	5	2	62.16	2	4.6712
Indoline	10,328	Indoles and derivatives	119.166	1.3351	-2.025	1	1	12.03	0	0.19917
Tubotaiwine	100,004	Strychnos alkaloids	324.423	2.3452	-3.568	4	1	41.57	3	1.5804
Cinchonidine	101,744	Cinchona alkaloids	294.397	2.6804	-3.079	3	1	36.36	3	0.88095
Tryptoline	107,838	Indoles and derivatives	172.23	1.2188	-2.39	2	2	27.82	0	1.1795
Alloyohimbine	120,716	Yohimbine alkaloids	354.448	2.3512	-3.065	5	2	65.56	2	1.5035
Cuscohygrine	1,201,543	Alkaloids and derivatives	224.347	1.2932	-1.22	3	0	23.55	4	4.2839
Sebiferine	10,405,046	Phenanthrenes and derivatives	341.406	1.9462	-2.753	5	0	48	3	5.7459
Condylocarpine	10,914,255	Strychnos alkaloids	322.407	2.2523	-3.304	4	1	41.57	2	0.29114
19,20-Dihydroakuammicine	11,023,792	Alkaloids and derivatives	324.423	2.3452	-3.568	4	1	41.57	3	2.1615
Lochnericine	11,382,599	Aspidospermatan-type alkaloids	352.433	1.5996	-3.538	5	1	54.1	3	2.3885
3-Isoajmalicine	11,416,867	Yohimbine alkaloids	352.433	2.2674	-3.141	5	1	54.56	2	2.6043
Vindolidin	11,618,751	Plumeran-type alkaloids	426.511	1.3936	-3.098	7	1	79.31	5	3.2845
Vincapusine	11,646,359	Alkaloids and derivatives	368.432	2.6409	-2.695	6	1	63.93	3	2.2856
Epibubialine	11,830,997	Azaspiredecane derivatives	221.255	-0.1874	-1.424	4	1	49.77	0	1.6204
Vindoline	11,953,805	Plumeran-type alkaloids	456.537	1.3236	-3.116	8	1	88.54	6	3.2845
1,2-Dihydrovomilenine	11,953,964	Ajmaline-sarpagine alkaloids	352.433	1.8244	-3.654	5	2	61.8	2	1.1872
Pericyclivine	11,969,544	Macroline alkaloids	322.407	2.8635	-3.038	4	1	45.33	2	0.20237
Lycocotnine	11,972,492	Prenol lipids	467.601	-0.1645	-1.824	8	3	100.85	6	0.56009
Cathanine	12,302,545	Aspidospermatan-type alkaloids	426.511	1.3713	-3.408	7	0	68.31	5	2.5051
Anahygrine	12,306,778	Alkaloids and derivatives	224.347	1.3823	-1.852	3	1	32.34	4	3.0573
Tabernaemontanin	12,309,360	Vobasan alkaloids	354.448	2.6197	-3.678	5	1	62.4	3	3.1533
4-Methoxynorsecurinine	101,091,319	Pyrrrolizidines	233.266	-0.0349	-1.324	4	0	38.77	1	1.5563
Akuammicine	101,281,350	Strychnos alkaloids	322.407	2.2523	-3.304	4	1	41.57	2	0.87991
Heterophyllisine	101,289,617	Quinolindines	375.507	1.5254	-3.175	5	1	59	2	4.4531
Geracranolide	101,616,641	Prenol lipids	266.336	2.1659	-2.371	4	2	66.76	0	1.5629
Isoajmaline	101,624,670	Ajmaline-sarpagine alkaloids	326.438	1.791	-3.484	4	2	46.94	1	3.4513
Hetidine	101,685,340	Prenol lipids	357.448	0.8838	-2.601	5	2	77.84	0	2.8009
Catharosine	101,686,461	Plumeran-type alkaloids	384.474	0.909	-2.688	6	2	73.24	3	3.3742
Fluorocarpamine	101,688,177	Carboxylic acids and derivatives	339.414	1.8706	-3.095	5	1	58.64	2	0.97774
Ajmalicine	101,927,009	Indoles and derivatives	370.447	3.0403	-3.438	6	1	63.93	2	2.2403
Hetisinone	101,930,090	Prenol lipids	327.423	1.0959	-2.903	4	2	60.77	0	0.86256
Rhazimol	101,986,486	Corynanthean-type alkaloids	338.406	0.2205	-2.55	5	2	73.13	2	2.6104
18-Hydroxy-3-epi-alpha-yohimbine	102,004,710	Yohimbine alkaloids	370.447	1.4991	-2.666	6	3	85.79	2	2.3334
Sarpagine	102,090,391	Macroline alkaloids	310.396	2.4395	-2.632	4	3	59.49	1	2.0345
Velbanamine	102,399,433	Indoles and derivatives	298.428	3.3453	-3.206	3	2	39.26	1	3.5116
Catharosine	2564-23-0	Plumeran-type alkaloids	384.474	0.909	-2.688	6	2	73.24	3	3.3742

GC813 inhibitor (AW4) showed binding energy of -8.0 kcal/mol. All the lead compounds established both a good number of hydrogen bonds as well as hydrophobic interactions with the target except 28,288,759 which exhibited only hydrophobic interactions. The lead molecules-DB06817 (Raltegravir), 120,716 (Alloyohimbine) and 11,969,544 (Pericyclivine) established hydrogen bond interactions with either His41 or Cys148 or both (catalytic dyad) which may explain their mode of inhibition against the enzyme target.

3.5. Common lead molecules as potential dual or triple inhibitors of the enzyme targets

Among the FDA approved antiviral drugs, we found that DB13879 (Glecaprevir) and DB09102 (Daclatasvir) can be potential

leads for dual inhibition of SARS-CoV-2 3CL^{pro} (Fig. 1A, B) and SARS-CoV 3CL^{pro} as they were common top 5 leads. The lead molecule DB09297 (Paritaprevir) can be explored as a dual inhibitor of SARS-CoV-2 3CL^{pro} (Fig. 1C) and MERS-CoV 3CL^{pro} and DB01072 (Atazanavir) can be used as an inhibitor for dual inhibition of SARS-CoV 3CL^{pro} and MERS-CoV 3CL^{pro}. While Glecaprevir, Daclatasvir and Paritaprevir have been used against chronic hepatitis C (For the Study of the Liver (KASL, K.A., others, 2018; Hézode, 2018), Atazanavir (HIV-1 protease inhibitor) is primarily used for the treatment of HIV infection (Eckhardt and Gulick, 2017). Interestingly, we found that the phytochemicals 11,646,359 (Vincapusine), 120,716 (Alloyohimbine) and 10,308,017 (Gummadiol) were common top 5 leads among the three targets and therefore, these phytochemicals can be used as triple inhibitors of SARS-CoV-2 3CL^{pro} (Fig. 2A–C), SARS-CoV 3CL^{pro} and MERS-CoV 3CL^{pro}.

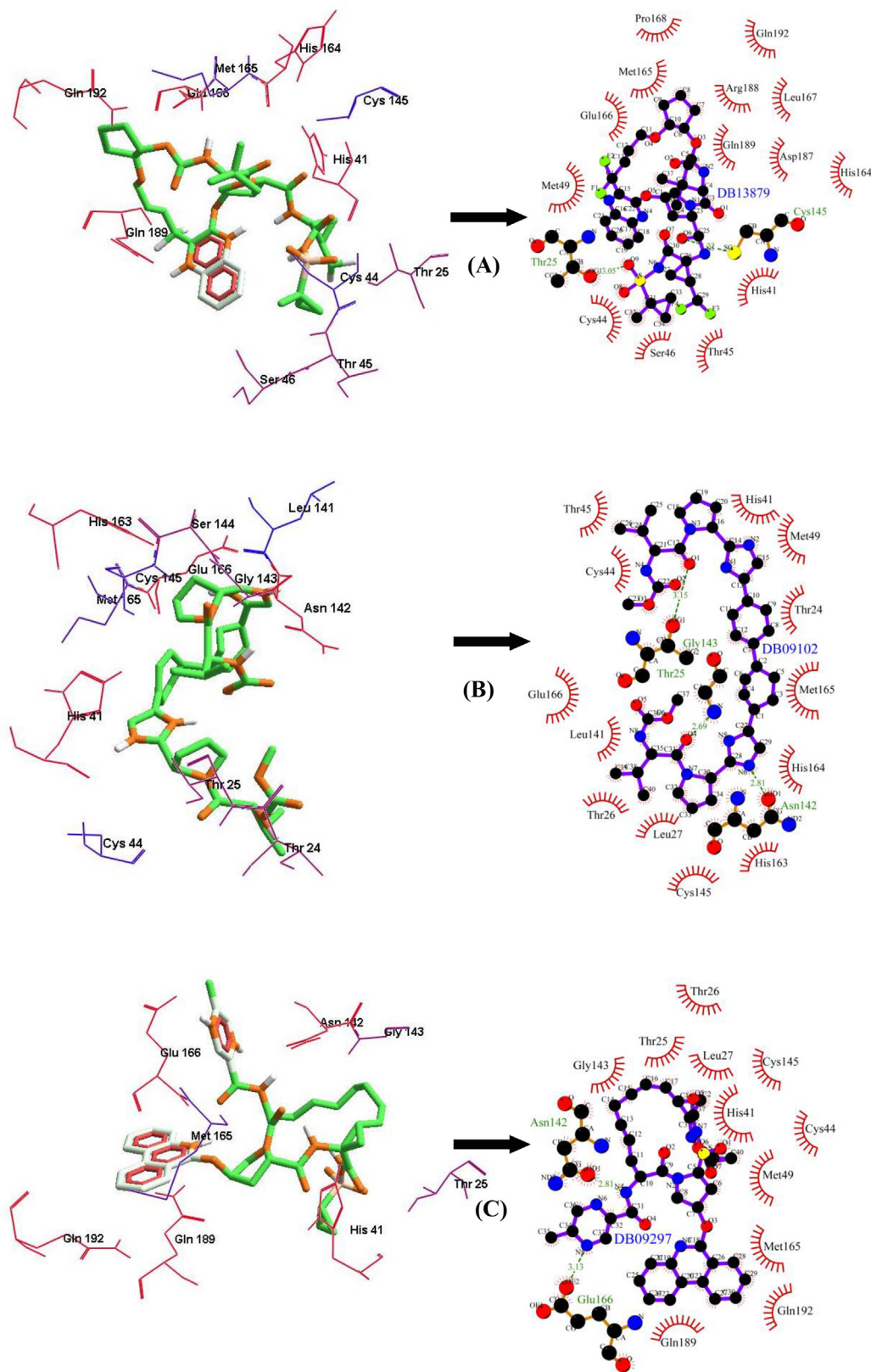


Fig. 1. The binding poses and LigPlot + results showing molecular interaction between SARS-CoV-2 3CL^{Pro} and lead molecules-(FDA approved antiviral drugs) (A) DB13879 (Glecaprevir) (B) DB09102 (Daclatasvir) (C) DB09297 (Paritaprevir). The hydrophobic interacting residues are indicated by red arcs with spikes and the green dashed lines with the bond distance correspond to hydrogen bonds.

The phytochemical 102,004,710 (18-Hydroxy-3-epi-alpha-yohimbine) was identified to be a potential dual inhibitor of SARS-CoV-2 3CL^{Pro} and SARS-CoV 3CL^{Pro}. Vinacapsine is a

β -amino alcohol-type alkaloid extracted from leaves of *Catharanthus pusillus*, a traditional medicinal plant of India believed to possess oncolytic properties (Khare, 2007). Gummadiol

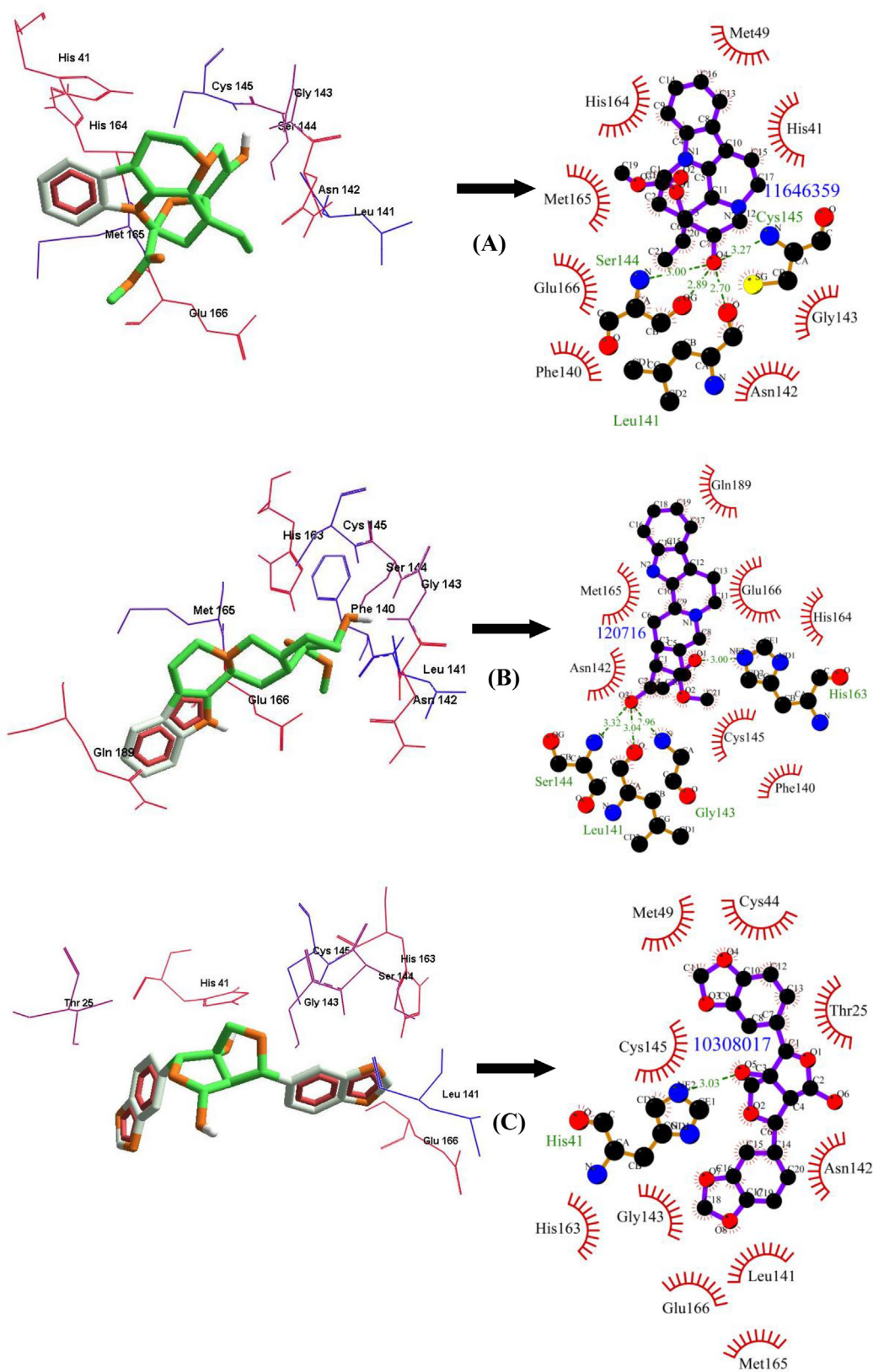


Fig. 2. The binding poses and LigPlot + results showing molecular interaction between SARS-CoV-2 3CLpro and lead molecules-(Phytochemicals) (A) 11,646,359 (Vincapusine) (B) 120,716 (Alloyohimbine) (C) 10,308,017 (Gummadiol). The hydrophobic interacting residues are indicated by red arcs with spikes and the green dashed lines with the bond distance correspond to hydrogen bonds.

belongs to the class of Furanoid lignans which can be extracted from *Gmelina arborea* (Anjaneyulu et al., 1975; Pathala et al.,

2015). Alloyohimbine and 18-Hydroxy-3-epi-alpha-yohimbine are alkaloids which are isomeric forms of yohimbine, an alkaloid

extracted from the bark of the tree *Pausinystalia yohimbe* and has been traditionally used for the treatment of sexual disorders (Anadón et al., 2016). However, the bioactivity of these compounds against viral infections have not been reported till date to the best of our knowledge and therefore these are novel phytochemical leads which could be further explored against coronavirus infections in humans. The key findings from the present study has been illustrated with Fig. 3.

4. Conclusion

The present work is an *in silico* attempt to propose lead molecules as potential inhibitors of coronavirus 3CL^{pro} enzyme. Our study unravels new chemical entities from a repertoire of

phytochemicals and FDA approved drugs that could be repurposed for treatment of coronavirus infection in humans. The leads suggested from this study could offer new candidate molecules in the drug discovery pipeline for the treatment and management of the disease. The current work is limited by small datasets and therefore, it would be worth exploring new chemical databases with big ligand sets for virtual screening procedure for identification of novel inhibitors against the target enzyme. A combined molecular docking and molecular dynamics simulation approach could be envisaged which would further provide useful mechanistic insights into the binding modes of inhibitions at the atomic level. Further research work is necessary to establish the inhibitory activity of the identified FDA approved lead molecules against the coronavirus 3CL^{pro} enzyme through *in vitro* and *in vivo* experiments.

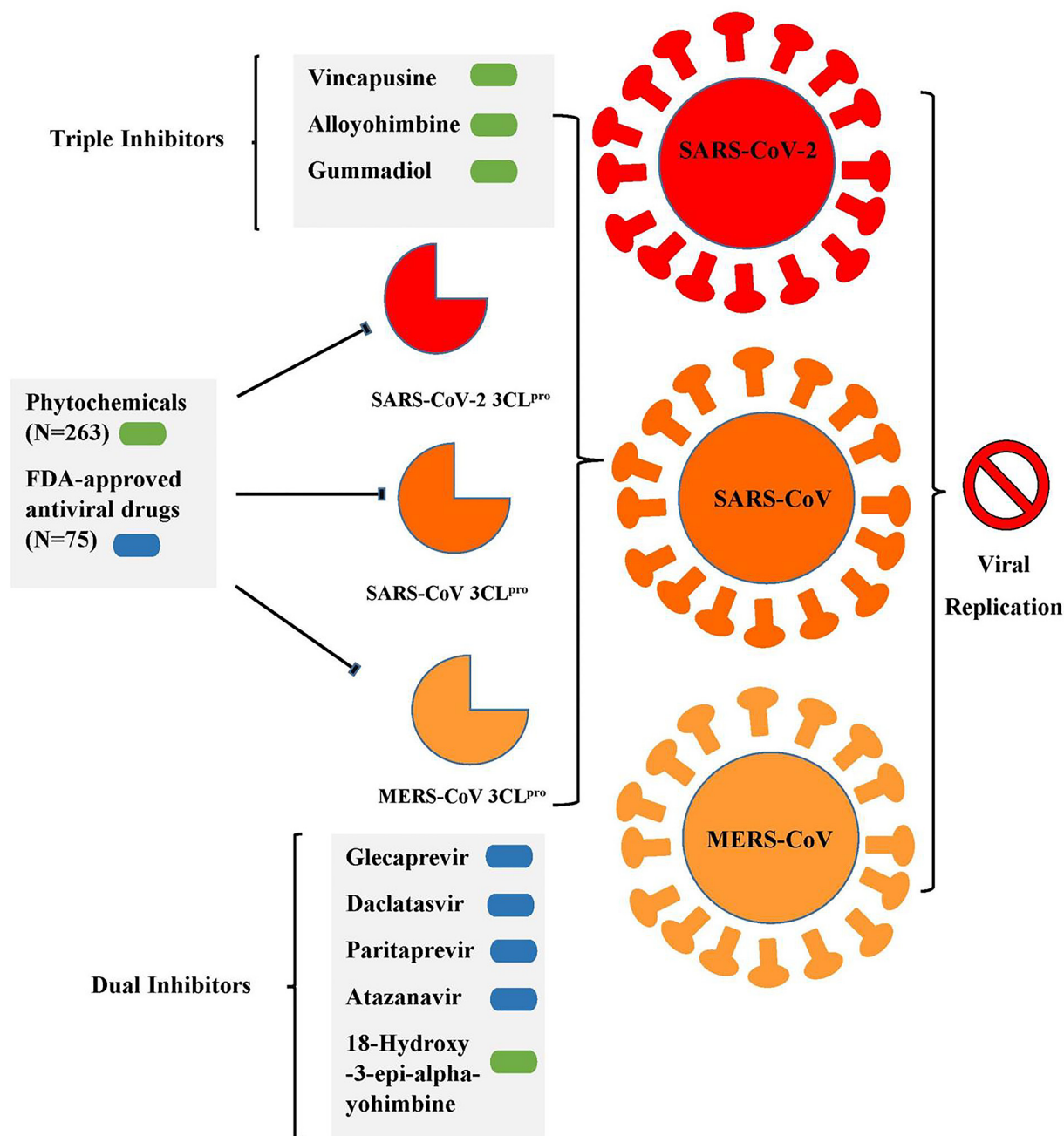


Fig. 3. A graphical summary illustrating the key findings from the present study.

Declaration of Competing Interest

The authors declare that they have no known competing financial interests or personal relationships that could have appeared to influence the work reported in this paper.

Acknowledgements

The authors would like to extend their sincere appreciation to the Researchers Supporting Project number (RSP-2019/154), King Saud University, Riyadh, Saudi Arabia. J. Lee thanks to Chungnam National University, Daejeon, Republic of Korea for the funding support. The authors thank the Deanship of Scientific Research and RSSU at King Saud University for their technical support.

References

- Abd El-Aziz, T.M., Stockand, J.D., 2020. Recent progress and challenges in drug development against COVID-19 coronavirus (SARS-CoV-2)-an update on the status. *Infect. Genet. Evol.* 83, 104327.
- Anadón, A., Martínez-Larrañaga, M.R., Ares, I., Martínez, M.A., 2016. Chapter 60 - Interactions between Nutraceuticals/Nutrients and Therapeutic Drugs, in: Gupta, R.C. (Ed.), *Nutraceuticals*. Academic Press, Boston, pp. 855–874. <https://doi.org/https://doi.org/10.1016/B978-0-12-802147-7.00060-7>.
- Anjaneyulu, A.S.R., Rao, A.M., Rao, V.K., Row, L.R., Pelter, A., Ward, R.S., 1975. The structure of gummadiol- α lignan hemi-acetal. *Tetrahedron Lett.* 16, 1803–1806.
- Bredenbeek, P.J., Pachuk, C.J., Noten, A.F.H., Charité, J., Luytjes, W., Weiss, S.R., Spaan, W.J.M., 1990. The primary structure and expression of the second open reading frame of the polymerase gene of the coronavirus MHV-A59; a highly conserved polymerase is expressed by an efficient ribosomal frameshifting mechanism. *Nucleic Acids Res.* 18, 1825–1832.
- Brian, D.A., Baric, R.S., 2005. Coronavirus genome structure and replication, in: *Coronavirus Replication and Reverse Genetics*. Springer, pp. 1–30.
- Cui, J., Li, F., Shi, Z.-L., 2019. Origin and evolution of pathogenic coronaviruses. *Nat. Rev. Microbiol.* 17, 181–192.
- Dhama, K., Sharun, K., Tiwari, R., Dadar, M., Malik, Y.S., Singh, K.P., Chaicumpa, W., 2020. COVID-19, an emerging coronavirus infection: advances and prospects in designing and developing vaccines, immunotherapeutics, and therapeutics. *Hum. Vaccin. Immunother.* 1–7.
- Eckhardt, B.J., Gulick, R.M., 2017. 152 - Drugs for HIV Infection, in: Cohen, J., Powderly, W.G., Opal, S.M. (Eds.), *Infectious Diseases (Fourth Edition)*. Elsevier, pp. 1293–1308.e2. <https://doi.org/https://doi.org/10.1016/B978-0-7020-6285-8.00152-0>.
- For the Study of the Liver (KASL, K.A., others, 2018. 2017 KASL clinical practice guidelines management of hepatitis C: Treatment of chronic hepatitis C. *Clin. Mol. Hepatol.* 24, 169–229.
- Forni, D., Cagliani, R., Clerici, M., Sironi, M., 2017. Molecular evolution of human coronavirus genomes. *Trends Microbiol.* 25, 35–48.
- Gorbalenya, A.E., 2001. Big nidovirus genome, in: *The Nidoviruses*. Springer, pp. 1–17.
- Graham, R.L., Donaldson, E.F., Baric, R.S., 2013. A decade after SARS: strategies for controlling emerging coronaviruses. *Nat. Rev. Microbiol.* 11, 836–848.
- Halgren, T.A., 1996. Merck molecular force field. I. Basis, form, scope, parameterization, and performance of MMFF94. *J. Comput. Chem.* 17, 490–519. [https://doi.org/10.1002/\(SICI\)1096-987X\(199604\)17:5<490::AID-JCC1>3.0.CO;2-P](https://doi.org/10.1002/(SICI)1096-987X(199604)17:5<490::AID-JCC1>3.0.CO;2-P).
- Hézode, C., 2018. Treatment of hepatitis C: results in real life. *Liver Int.* 38, 21–27.
- Jo, S., Kim, S., Shin, D.H., Kim, M.-S., 2020. Inhibition of SARS-CoV 3CL protease by flavonoids. *J. Enzyme Inhib. Med. Chem.* 35, 145–151.
- Khare, C.P., 2007. *Vinca pusilla* Murr., in: Khare, C.P. (Ed.), *Indian Medicinal Plants: An Illustrated Dictionary*. Springer New York, New York, NY, p. 1. https://doi.org/10.1007/978-0-387-70638-2_1743.
- Lacroix, A., Duong, V., Hul, V., San, S., Davun, H., Omaliss, K., Chea, S., Hassanin, A., Theppangna, W., Silihamavong, S., et al., 2017. Genetic diversity of coronaviruses in bats in Lao PDR and Cambodia. *Infect. Genet. Evol.* 48, 10–18.
- Lai, M.M.C., 2001. Coronaviridae: the viruses and their replication. In *Fields Virology*, Fourth Edition (Knipe DM, Howley PM, eds), Lippincott Williams and Wilkins, Philadelphia, pp. 1163–1185.
- Laskowski, R.A., Swindells, M.B., 2011. LigPlot+: multiple ligand-protein interaction diagrams for drug discovery. *J. Chem. Inf. Model.* 51, 2778–2786. <https://doi.org/10.1021/ci200227u>.
- Lee, H.-J., Shieh, C.-K., Gorbalenya, A.E., Koonin, E.V., La Monica, N., Tuler, J., Bagdzhadzhyan, A., Lai, M.M.C., 1991. The complete sequence (22 kilobases) of murine coronavirus gene 1 encoding the putative proteases and RNA polymerase. *Virology* 180, 567–582.
- Lipinski, C.A., 2004. Lead- and drug-like compounds: the rule-of-five revolution. *Drug Discov. Today. Technol.* 1, 337–341. <https://doi.org/10.1016/j.ddtec.2004.11.007>.
- Lundstrom, K., 2020. Coronavirus Pandemic—Therapy and Vaccines. *Biomedicines* 8, 109.
- Mohanraj, K., Karthikeyan, B.S., Vivek-Ananth, R.P., Chand, R.P.B., Aparna, S.R., Mangalapandi, P., Samal, A., 2018. IMPPAT: A curated database of Indian Medicinal Plants, Phytochemistry and Therapeutics. *Sci. Rep.* 8, 1–17.
- Morris, G.M., Huey, R., Lindstrom, W., Sanner, M.F., Belew, R.K., Goodsell, D.S., Olson, A.J., 2009. AutoDock4 and AutoDockTools4: automated docking with selective receptor flexibility. *J. Comput. Chem.* 30, 2785–2791. <https://doi.org/10.1002/jcc.21256>.
- Needle, D., Lountos, G.T., Waugh, D.S., 2015. Structures of the Middle East respiratory syndrome coronavirus 3C-like protease reveal insights into substrate specificity. *Acta Crystallogr. Sect. D Biol. Crystallogr.* 71, 1102–1111.
- O’Boyle, N.M., Banck, M., James, C.A., Morley, C., Vandermeersch, T., Hutchison, G.R., 2011. Open Babel: An open chemical toolbox. *J. Cheminform.* 3, 33. <https://doi.org/10.1186/1758-2946-3-33>.
- Padron-Regalado, E., 2020. Vaccines for SARS-CoV-2: lessons from other coronavirus strains. *Infect. Dis. Ther.* 9, 255–274.
- Pathala, D., Harini, A., Hegde, P.L., 2015. A review on gambhari (Gmelina arborea Roxb.). *J. Pharmacogn. Phytochem.* 4, 127–132.
- Sander, T., Freyts, J., von Korff, M., Rufener, C., 2015. DataWarrior: an open-source program for chemistry aware data visualization and analysis. *J. Chem. Inf. Model.* 55, 460–473. <https://doi.org/10.1021/ci500588j>.
- Simas, P.V.M., de Souza Barnabé, A.C., Durães-Carvalho, R., de Lima Neto, D.F., Caserta, L.C., Artacho, L., Jacomassa, F.A.F., Martini, M.C., dos Santos, M.M.A.B., Felipe, P.A.N., et al., 2015. Bat coronavirus in Brazil related to appalachian ridge and porcine epidemic diarrhea viruses. *Emerg. Infect. Dis.* 21, 729–731.
- Su, S., Wong, G., Shi, W., Liu, J., Lai, A.C.K., Zhou, J., Liu, W., Bi, Y., Gao, G.F., 2016. Epidemiology, genetic recombination, and pathogenesis of coronaviruses. *Trends Microbiol.* 24, 490–502.
- Trott, O., Olson, A.J., 2010. AutoDock Vina: improving the speed and accuracy of docking with a new scoring function, efficient optimization, and multithreading. *J. Comput. Chem.* 31, 455–461. <https://doi.org/10.1002/jcc.21334>.
- Veber, D.F., Johnson, S.R., Cheng, H.-Y., Smith, B.R., Ward, K.W., Kopple, K.D., 2002. Molecular properties that influence the oral bioavailability of drug candidates. *J. Med. Chem.* 45, 2615–2623.
- Weiss, S.R., Navas-Martin, S., 2005. Coronavirus pathogenesis and the emerging pathogen severe acute respiratory syndrome coronavirus. *Microbiol. Mol. Biol. Rev.* 69, 635–664.
- Wishart, D.S., Knox, C., Guo, A.C., Cheng, D., Shrivastava, S., Tzur, D., Gautam, B., Hassanali, M., 2008. DrugBank: a knowledgebase for drugs, drug actions and drug targets. *Nucleic Acids Res.* 36, D901–D906.
- Woo, P.C.Y., Lau, S.K.P., Lam, C.S.F., Lau, C.C.Y., Tsang, A.K.L., Lau, J.H.N., Bai, R., Teng, J.L.L., Tsang, C.C.C., Wang, M., et al., 2012. Discovery of seven novel mammalian and avian coronaviruses in the genus deltacoronavirus supports bat coronaviruses as the gene source of alphacoronavirus and betacoronavirus and avian coronaviruses as the gene source of gammacoronavirus and deltacoronavi. *J. Virol.* 86, 3995–4008.
- Wu, F., Zhao, S., Yu, B., Chen, Y.-M., Wang, W., Song, Z.-G., Hu, Y., Tao, Z.-W., Tian, J.-H., Pei, Y.-Y., et al., 2020. A new coronavirus associated with human respiratory disease in China. *Nature* 579, 265–269.
- Zhou, P., Yang, X.-L., Wang, X.-G., Hu, B., Zhang, L., Zhang, W., Si, H.-R., Zhu, Y., Li, B., Huang, C.-L., et al., 2020. A pneumonia outbreak associated with a new coronavirus of probable bat origin. *Nature* 579, 270–273.
- Ziebuhr, J., 2005. The coronavirus replicase, in: *Coronavirus Replication and Reverse Genetics*. Springer, pp. 57–94.
- Ziebuhr, J., Thiel, V., Gorbalenya, A.E., 2001. The autocatalytic release of a putative RNA virus transcription factor from its polyprotein precursor involves two paralogous papain-like proteases that cleave the same peptide bond. *J. Biol. Chem.* 276, 33220–33232.